J. Phys. B: At. Mol. Phys. **20** (1987) 5505-5515. Printed in the UK

Total electron scattering cross sections for argon, krypton and xenon at low electron energies

K P Subramanian and Vijay Kumar

Physical Research Laboratory, Navrangpura, Ahmedabad-380009, India

Received 19 May 1987, in final form 13 July 1987

Abstract. Absolute electron scattering cross sections for argon, krypton and xenon have been measured at low electron energies using the powerful technique of photoelectron spectroscopy. The measurements have been carried out at electron energies varying from 0.7 to 10 eV with an accuracy of ±2.7%. The cross sections obtained in the present paper have been compared with other recent measurements and theoretical computations.

1. Introduction

The scattering of low-energy electrons by atoms and molecules has been studied for many years. Interest in both experimental as well as theoretical aspects of the subject has grown enormously in the last decade. One of the reasons for this interest is that new theoretical models for calculating scattering cross sections accurately are now available in the literature with the result that a direct comparison with experimental data is now possible. Electron scattering at low energies is also important for the better understanding of weakly ionised plasmas, e.g. gas discharges, planetary atmospheres and interstellar clouds. Such knowledge also helps to enlarge the scope of many fields like gaseous dielectrics and diffuse-discharge switching.

In recent years, the electron scattering cross section measurements for argon, krypton and xenon have been carried out using various new techniques while theoretical data obtained using better approximations have also been available for these noble gases. The latest measurements in the case of electron-argon scattering cross sections have been made by Kauppila *et al* (1976, 1977) and Nickel *et al* (1985) using transmission techniques in the electron energy regions 0.4-30 and 4-300 eV respectively. Using a time-of-flight technique, Charlton *et al* (1980) and Ferch *et al* (1985) obtained total cross sections at electron energies ranging from 2-50 and 0.08-20 eV respectively. In another experiment, using a linearised Ramsauer technique, Jost *et al* (1983) have measured cross sections at a number of electron energies between 0.08 and 60 eV. Electron scattering cross sections for argon have also been computed by McEachran and Stauffer (1983) and Dasgupta and Bhatia (1985) using the dipole part of the polarisation potential and treating exchange exactly, and using the method of polarised orbitals, respectively. R-matrix calculations have been reported by Fon *et al* (1983) and Bell *et al* (1984) in the electron energy regions 3-150 and 0-19 eV respectively. Using Kohn-Sham-type one-particle theory, Haberland *et al* (1986) have reported scattering cross sections for argon at only two energies below 10 eV. Out of the experimental data available, it appears that the cross section values reported by Jost *et al* and Nickel *et al* seem to match each other reasonably well. The theoretically

0022-3700/87/205505+11$02.50

calculated cross sections by the R-matrix method (Fon *et al* 1983, Bell *et al* 1984) and by the method of polarised orbitals (Dasgupta and Bhatia 1985) compare favourably with the experimental data mentioned above while computed cross sections given by McEachran and Stauffer (1983) are very much on the high side.

Electron–krypton scattering cross section measurements have, in recent years, been carried out by Dababneh *et al* (1980) and Jost *et al* (1983) in the electron energy regions 1.9–100 and 0.3–60 eV using a transmission technique and the linearised Ramsauer method respectively. Latest theoretical values for cross sections have been reported by McEachran and Stauffer (1984), Fon *et al* (1984) and Haberland *et al* (1986) using similar techniques as for argon, while Sin Fai Lam (1982) reported cross sections taking into account direct and indirect relativistic effects. The measured cross section values reported by Jost *et al* and Dababneh *et al* match well in the electron energy region 2–7 eV but at higher energies, Dababneh *et al* have reported much lower values. Compared with this, there is a large discrepancy between cross section data theoretically computed by the investigators mentioned above and values reported through experimental measurements.

Electron scattering cross sections for xenon have lately been measured by Dababneh *et al* (1980), Jost *et al* (1983, 1984) and Nickel *et al* (1985) in the electron energy regions 2.8–50, 0.1–60 and 4–300 eV respectively. Theoretically computed cross sections have also been reported by McEachran and Stauffer (1984), Sin Fai Lam (1982) and Haberland *et al* (1986) using the methods discussed above. The measured values of cross sections by Jost *et al*, Nickel *et al* and Dababneh *et al* match extremely well at electron energies below 5 eV, but at energies between 5 and 10 eV, the values given by Jost *et al* are much higher than those reported by other investigators. The theoretical values of Sin Fai Lam (1982) match favourably with the experimental cross sections up to only 2 eV. At energies larger than 2 eV the computed cross sections of Sin Fai Lam (1982) and McEachran and Stauffer (1984) are much higher than the measured values while the values reported by Haberland *et al* (1986) are much lower.

In the light of the arguments discussed above, it is clear that more measurements in this direction are needed, possibly using new techniques. In the present experiment, absolute electron scattering cross sections have been measured for argon, krypton and xenon at low electron energies from 0.7 to 10 eV using the powerful technique of photoelectron spectroscopy. Recently, absolute electron–helium and electron–neon scattering cross sections were measured by the authors in the same electron energy range using the same technique (Kumar *et al* 1987). The present paper is an attempt to complete the electron scattering cross section measurements for noble-gas atoms at low electron energies.

2. Experimental set-up

The experimental set-up for the measurement of electron scattering cross sections using a photoelectron source has been discussed in detail elsewhere (Kumar *et al* 1987). A brief description is being given here for the sake of completeness. Electrons are produced by photoionisation of a source gas like argon, krypton or xenon in a small ionisation region located close to the electron energy analyser. Vacuum ultraviolet photons from strong atomic emission lines are allowed to impinge on the source gas, which is photoionised and electrons of two energies corresponding to $^2P_{1/2}$ and $^2P_{3/2}$ states of the ion are produced. With photons of a single wavelength and using one

source gas at a time, two electron energies would be accessible. With the various combinations of photons of three different wavelengths (HeI 58.4, NeI 73.6 and 74.4 nm) and argon, krypton and xenon as source gases, 18 electron energies are accessible from 0.7 to 10 eV. Two of the electron energies are very close to each other and cannot be resolved, with the result that only 17 electron energies are available for carrying out the scattering studies. The resonant emission lines HeI (58.4 nm) and NeI (73.6 and 74.4 nm) are produced by microwave discharge of helium and neon respectively. The intensity of the photon beam is monitored using a beam splitter which consists of a high transparency wire mesh mounted at an angle of 45° to the beam axis. More than 90% of the light is transmitted and the rest is reflected towards a light detector which includes a perspex light pipe coated at the front end with a scintillator, p-terphenyl, and an EMI 6199 photomultiplier. Any change in the light intensity could thus be monitored using the beam splitter, and the change in intensity, if any, during the experiment could be incorporated in the results. The beam splitter system enclosed in a stainless chamber is evacuated by a diffstak pump (700 l s^{-1}) and backed by a rotary pump of appropriate pumping speed.

The VUV photon beam was allowed to pass through a large number of circular baffles before emerging into a small region where photoionisation of the source gas takes place. The pressure of the source gas was kept low to avoid any electron scattering by the source-gas atoms. The photoelectrons thus produced were energetically analysed using a cylindrical mirror analyser (CMA) and were detected by a channeltron (Mullard B419 BL) operated in the counting mode. After proper amplification, the signals were stored in a home-made microprocessor-controlled multichannel analyser operated in the multiscaling mode. The ionisation region, the accelerating and the analysing regions of the CMA and the channeltron region were differentially pumped by a fast diffstak pump (2000 l s^{-1}), backed by a mechanical pump of appropriate pumping speed.

The CMA has a slit-to-slit focusing geometry and the diameters of the inner and outer cylinders were 10.2 and 25.4 cm respectively. The photoelectrons produced in the ionisation region were allowed to enter the first slit of the analyser at an angle of $54°44' \pm 3°$. The distance between the two slits was kept at 15.9 cm, in accordance with the best focusing conditions around 55°. A slit width of 2 mm was used for both slits.

The photoelectrons produced in the small ionising region by the interaction of monochromatic VUV photons with the source gas at low pressure were allowed to be scattered by the target gas. The scattering path length, limited between the centre and the slit of the ionising region over 2π geometry, was 2.37 cm. Without any target gas, the amplitudes of the photoelectron peaks produced by the source gas were monitored at a fixed but low source-gas pressure in the ionisation region. The target gas was then introduced and if the source gas and target gas were not the same (e.g. when source gas was argon and target gas was krypton or xenon), the amplitudes of the photoelectron peaks would decrease with increasing target-gas pressure. This decrease was attributed to electron scattering by target-gas species whose number density increases with increasing pressure. When the source and target gases were the same (e.g. when source gas is argon and it is required to measure electron scattering cross section for argon itself), the amplitudes of photoelectron peaks would first increase with increase of source/target-gas pressure and after a certain gas pressure was attained, the amplitudes would start decreasing with subsequent increase in target-gas pressure. To begin with, the increase in peak amplitudes would be due to the increase in photoelectron production rate followed by small electron scattering, but the subsequent decrease in amplitudes was because of electron scattering alone.

The absolute gas pressure in the ionisation and scattering regions was measured using an MKS capacitance manometer (head 310 MH − 1). The details about pressures in different regions of the instrument and the performance of the photoelectron spectrometer have been given in our previous publication (Kumar *et al* 1987).

3. Method

Different analysis procedures have been used, depending on the nature of the source and target atoms. In the present experiment, the source atoms used for producing photoelectrons were argon, krypton and xenon while the target atoms involved in the measurement of scattering cross sections, incidentally, were also argon, krypton and xenon. The method followed when the source and target atoms are different was discussed in our previous publication (Kumar *et al* 1987). This method will be discussed briefly here again and extended to the case when the source and target atoms are the same.

3.1. When source and target atoms are different

When a beam of electrons is passing through a scattering medium, the transmitted intensity is given by

$$I_e = I_{e0} \exp(-n\sigma x)$$

where I_{e0} is the initial intensity of the electrons, n is the number density of the target atoms, x is the scattering path length and σ is the total electron scattering cross section at a particular energy. In the experiment, I_{e0} and I_e are the amplitudes of the photoelectron peaks at a single electron energy before and after the electron scattering respectively.

The pressure of the source gas inside and outside the ionising regions are P' and p' respectively, which remained constant throughout the experiment, while P and p are pressures of the target gas inside and outside the ionising region. At two pressures P_1 and P_2 of the target gas, the amplitudes of the photoelectron peak are given by

$$I_{e1} = I_{e01} \exp[-(P' + P_1) n_0 \sigma x/760]$$

$$I_{e2} = I_{e02} \exp[-(P' + P_2) n_0 \sigma x/760]$$

where n_0 is the Loschmidt number. The ratio of the observed peak amplitudes at the two different pressures are given by

$$I_{e1}/I_{e2} = (I_{e01}/I_{e02}) \exp[-(P_1 - P_2) n_0 \sigma x/760] \ldots . \tag{1}$$

The electrons produced in the small photoionisation region relate to the average photon intensity $\langle I_\lambda \rangle$ and the pressure:

$$I_{e01}/I_{e02} = P'\langle I_\lambda \rangle_1 / P'\langle I_\lambda \rangle_2 = \langle I_\lambda \rangle_1 / \langle I_\lambda \rangle_2$$

$$= I_{\lambda 01}/I_{\lambda 02} \exp[-(k/760)(P_1 - P_2)(al_1 + l_2)] \ldots \tag{2}$$

where k and k' are the photoabsorption coefficients of the target and sources gases respectively at a particular photon wavelength. k' is eliminated in ratio (2) of I_{e01} to I_{e02}. $I_{\lambda 01}$ and $I_{\lambda 02}$ are the incident photon intensities at pressures P_1 and P_2. The factor a is the ratio of pressures p and P, which have been defined earlier. The pressure

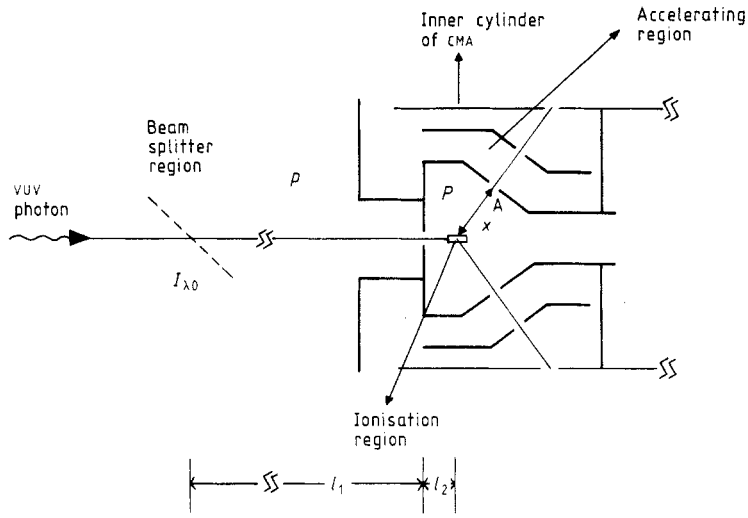

Figure 1. Schematic diagram showing ionisation as well as the electron scattering region in the cylindrical mirror analyser of the photoelectron spectrometer.

measurements of P and p over a range $0.025\text{-}10^{-3}$ Torr indicated that the factor a was constant throughout this pressure range. The lengths l_1, l_2 are shown in figure 1. The value of a was found to be 0.124 while the lengths l_1, l_2 and x from the geometry of the apparatus were 30, 2.58 and 2.37 cm respectively.

Substituting equation (2) into equation (1) and simplifying, one obtains

$$\ln\left(\frac{I_{e2}I_{\lambda 01}}{I_{e1}I_{\lambda 02}}\right)=\left(\frac{P_1-P_2}{760}\right)[n_0\sigma x+k(al_1+l_2)] \tag{3}$$

for which the ratio of $I_{\lambda 01}$ to $I_{\lambda 02}$ could be determined from the beam splitter.

3.2. When source and target atoms are the same

In this case where source and target atoms are the same, analysis is almost similar to that in § 3.1. However, the terms I_{e01} and I_{e02} become pressure dependent such that

$$I_{e01}/I_{e02}=P_1\langle I_\lambda\rangle_1/P_2\langle I_\lambda\rangle_2.$$

Making the correction for the photoabsorption on the same lines as given in § 3.1, the final equation would be

$$\ln\left(\frac{I_{e2}I_{\lambda 01}P_1}{I_{e1}I_{\lambda 02}P_2}\right)=\left(\frac{P_1-P_2}{760}\right)[n_0\sigma x+k(al_1+l_2)]. \tag{4}$$

4. Error analysis

All errors in the measurement of electron scattering cross sections have been discussed in detail previously (Kumar *et al* 1987). Errors in pressure, temperature or scattering path length, errors due to counting statistics, and cross section shape errors caused by forward scattering of electrons, gas impurities and uncertainty in the incident electron energy, have been dealt with at length in our previous publication. In the present experiment, the most probable error was estimated to be ±2.7%.

5. Results and discussion

The electron scattering cross sections for argon, krypton and xenon were measured using equations (3) when source and target atoms were different and equation (4) when source and target atoms were the same. In equations (3) and (4), all the parameters I_{e1}, I_{e2}, $I_{\lambda 01}$, $I_{\lambda 02}$, P_1 and P_2 could be determined experimentally and the cross section σ could be calculated.

5.1. Argon

The total electron-argon scattering cross sections are shown in figure 2 for electron energies ranging from 0.7 to 10 eV along with error bars at two electron energies only. Also shown in the figure are the measured cross sections reported by Jost *et al* (1983), Nickel *et al* (1985), Ferch *et al* (1985) and Charlton *et al* (1980). However, cross sections obtained by Kauppila *et al* (1976, 1977) have not been included in the figure due to lack of space. Theoretically computed cross sections by Fon *et al* (1983), Dasgupta and Bhatia (1985) and Haberland *et al* (1986) have also been shown in figure 2 while results reported by Bell *et al* (1984) and McEachran and Stauffer (1983) could not be shown. The cross sections by McEachran and Stauffer have been computed at four energies only between 3 and 10 eV and the values are higher by about 6-35% as compared with results obtained in the present experiment. Both Bell *et al* and Fon *et al* have computed the cross section by the R-matrix method and the values of cross

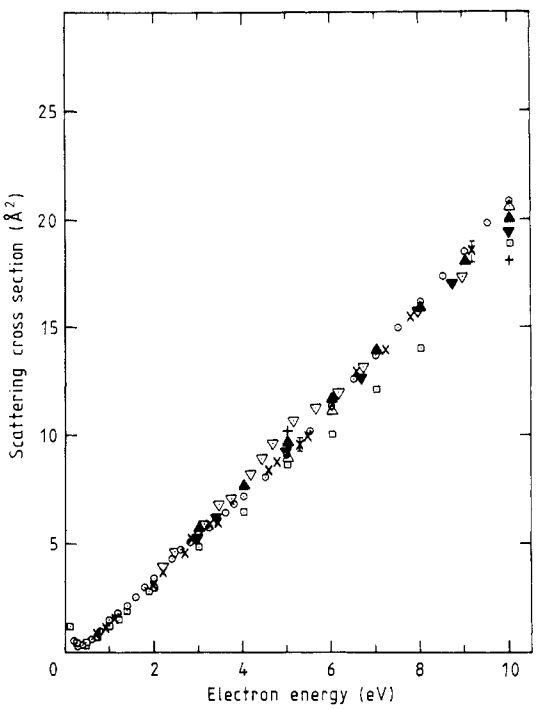

Figure 2. Total electron-argon scattering cross sections as a function of incident electron energy from 0.7 to 10 eV; ⊙, Jost *et al* (1983); △, Nickel *et al* (1985); ⊡, Ferch *et al* (1985); ▽, Charlton *et al* (1980); ▲, Fon *et al* (1983); ▼, Dasgupta and Bhatia (1985); +, Haberland *et al* (1986); ×, present results.

sections by these investigators are very close to each other at electron energies between 3 and 10 eV. For this reason, the cross section data of Fon *et al* only have been retained for further discussion later on.

The scattering cross sections for argon as measured by Nickel *et al* (1985) have been reported at five electron energies between 4 and 10 eV. However, cross sections at only three representative electron energies have been shown in figure 2. The values of cross sections by Nickel *et al* (1985) and Jost *et al* (1983) at a larger number of energy points between 0 and 10 eV are comparable to the results obtained in the present experiment within the stipulated experimental errors. The cross sections by Charlton *et al* (1980) between 2 and 10 eV are in good agreement with our results in the energy ranges 2-3.5 and 6.5-9 eV, but in the energy region 3.5-6.5 eV, the cross sections reported by Charlton *et al* are higher to a maximum of 12% at 5 eV. There is excellent agreement between the cross section values at electron energies up to 2 eV measured by Ferch *et al* and those reported in the present experiment. At higher energies, the results quoted by Ferch *et al* are lower to the extent of about 10 and 15% at 6 and 8 eV respectively. The theoretically computed cross sections by the R-matrix method (Fon *et al* 1983) and the polarised orbital method (Dasgupta and Bhatia 1985) at electron energies between 3 and 10 eV match extremely well with the measured values obtained in the present paper. Haberland *et al* (1986) have computed scattering cross sections for argon at two energy points below 10 eV. The cross section at 5 eV energy agrees well with that obtained in the present paper, while at 10 eV electron energy, the computed value of the cross section is quite low.

5.2. Krypton

The total electron scattering cross sections for krypton as measured in the present experiment are shown in figure 3 for electron energies between 0.7 and 10 eV. The results of the present experiment are shown along with the values of the measured cross sections reported by Dababneh *et al* (1980) and Jost *et al* (1983) and theoretically computed results by Sin Fai Lam (1982), Fon *et al* (1984) and Haberland *et al* (1986). In this figure, we have not included the result reported by McEachran and Stauffer (1984) obtained with an adiabatic exchange approximation because these are much higher than those reported in the present paper. The difference in values of cross sections in the two cases varies from about 15 to 50% at energies below 10 eV with a maximum discrepancy of about 50% at 7.5 eV.

The total electron-krypton scattering cross sections obtained in the present experiment are in excellent agreement with cross sections measured by Jost *et al* (1983) and Dababneh *et al* (1980) in the electron energy region up to 5 eV. The values of cross sections measured in the present paper are lower by 6-11% at electron energies between 6 and 10 eV as compared with those reported by Jost *et al* and by 5-4% as compared with values given by Dababneh *et al.* There is reasonably good agreement between the measured results in the present paper and the computed values of cross sections given by Sin Fai Lam (1982) at electron energies up to 2 eV, but at higher energies, the cross sections reported by Sin Fai Lam are very large. Haberland *et al* (1986) have computed the cross sections at two electron energies only; at 5 eV, the value of the cross section matches well with that measured in the present work, but at 10 eV, the cross section value is much lower. Fon *et al* (1984), using the R-matrix method, have reported cross sections at a large number of energy points between 1 and 10 eV. The values of cross sections reported by them are systematically large by more than 30-18%

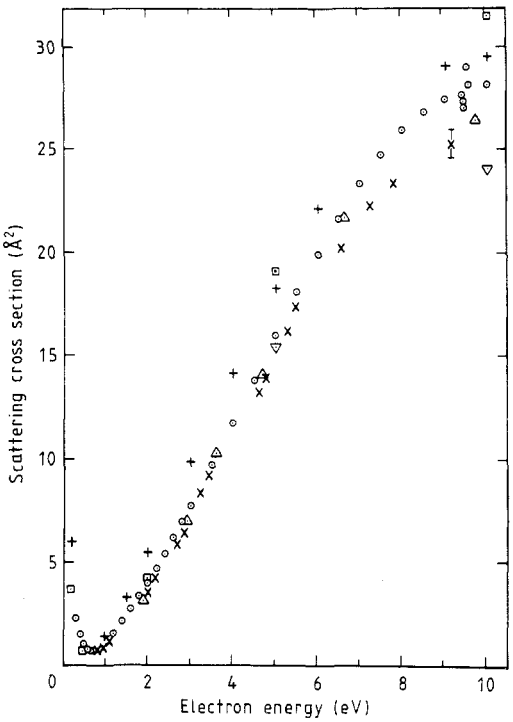

Figure 3. Total electron-krypton scattering cross sections as a function of incident electron energy from 0.7 to 10 eV; ⊙, Jost *et al* (1983); △, Dababneh *et al* (1980); ⊡, Sin Fai Lam (1982); ▽, Haberland *et al* (1986); +, Fon *et al* (1984); ×, present results.

at energies between 1 and 10 eV as compared with those obtained in the present paper. However, the shape of the cross section curve in the two cases is similar.

5.3. Xenon

The total electron scattering cross section for xenon measured in the present experiment are shown in figure 4 for electron energies between 0.7 and 10 eV. Also shown in the figure are the measured cross sections reported by Jost *et al* (1983, 1984), Dababneh *et al* (1980) and Nickel *et al* (1985) and the theoretically computed cross sections by Sin Fai Lam (1982) and Haberland *et al* (1986). The previously measured cross sections by Jost *et al* (1983) were thoroughly revised by them later on (Jost *et al* 1984) and only the revised values of cross sections have been included in figure 4. As in the case of argon and krypton, the cross sections given by McEachran and Stauffer (1984) for xenon have not been shown in the figure as these are very large in comparison with the results obtained in the present experiment.

The scattering cross section values as measured by Nickel *et al* (1985) have been reported only at five electron energies between 4 and 10 eV while there are eight values of cross sections given by Dababneh *et al* (1980) at electron energies between 2.8 and 10 eV as against the large number of data points reported by Jost *et al* (1984). The scattering cross sections obtained in the present paper are in fairly good agreement with those reported by Nickel *et al* and Dababneh *et al* throughout the energy region varying from 0.73 to 10 eV except for a small region between 5.5 and 7.5 eV where the

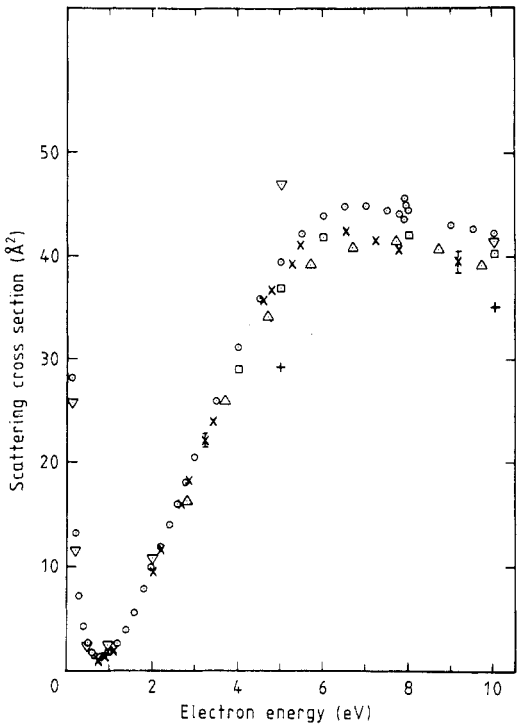

Figure 4. Total electron-xenon scattering cross sections as a function of incident electron energy from 0.7 to 10 eV; ⊙, Jost *et al* (1983); △, Dababneh *et al* (1980); ⊡, Nickel *et al* (1985); ▽, Sin Fai Lam; +, Haberland *et al* (1986); ×, present results.

cross section values by Dababneh *et al* are slightly lower. There is excellent agreement between the cross section values obtained in the present paper and those given by Jost *et al* (1984) for electron energies up to 5.5 eV, but at higher electron energies, the values given by Jost *et al* are higher by 6–9% at energies between 6.5 and 9.5 eV. The theoretically computed cross sections of Sin Fai Lam (1982) match favourably with those reported in the present paper at electron energies up to 2 eV only, but the cross section values reported at 10 and 5 eV are slightly higher and very large respectively. Haberland *et al* (1986) have reported cross sections at 5 and 10 eV only and the values of cross sections are much lower than those obtained in the present paper.

The values of cross sections for argon, krypton and xenon as measured in the present experiment have been given in table 1.

6. Conclusion

From the results discussed above, it is clear that the values of electron scattering cross sections for argon, krypton and xenon as measured in the present experiment may be better than those reported by other investigators. Firstly, the accuracy of the measurement of ±2.7% as estimated in the present experiment is definitely better than that reported by many other investigators. Secondly, the number of energy points at which cross sections have been measured in the present paper is many times larger than that reported in a few other experiments. It may be pointed out here that at low electron

Table 1. Total electron scattering cross sections for agron, krypton and xenon as measured in the present paper.

Electron energy (eV)	Electron scattering cross sections (Å^2)		
	Argon	Krypton	Xenon
0.73	0.96	0.74	1.10
0.91	1.20	0.90	1.28
1.09	1.54	1.19	1.90
2.00	3.09	3.54	9.58
2.18	3.66	4.17	11.69
2.66	4.60	5.79	16.01
2.85	5.23	6.36	18.28
3.23	5.90	8.33	22.13
3.41	6.04	9.14	23.91
4.59	8.41	13.10	35.57
4.77	8.81	13.84	36.47
5.28	9.58	16.12	39.09
5.46	9.96	17.31	40.86
6.55	12.93	20.17	42.33
7.22	13.90	22.20	41.38
7.78	15.41	23.29	40.54
9.14	18.45	25.20	39.27

energies, the photoelectron source is better than the conventional electron gun source in at least two respects; the energy of the photoelectron peak is defined with higher accuracy and the energy spread of the peak (FWHM) is much smaller.

It is also evident that the precise theoretical calculations to reproduce the measured electron scattering cross sections for krypton and xenon are still not available. However, the computations by the R-matrix method and polarised orbital technique used by Fon *et al* (1983) and Dasgupta and Bhatia (1985) could faithfully reproduce the measured values of the cross sections for argon in the electron energy region below 10 eV. It is, therefore, stressed that more theoretical work needs to be carried out in this direction.

Acknowledgment

The authors would like to thank Dr V B Sheorey for useful discussions during the experiment.

References

Bell K L, Scott N S and Lennon M A 1984 *J. Phys. B: At. Mol. Phys.* **17** 4757-65

Charlton M, Griffith T C, Heyland G R and Twomey T R 1980 *J. Phys. B: At. Mol. Phys.* **13** L239-44

Dababneh M S, Kauppila W E, Downing J P, Laperriere F, Pol V, Smart J H and Stein T S 1980 *Phys. Rev.* **22A** 1872-77

Dasgupta A and Bhatia A K 1985 *Phys. Rev.* A **32** 3335-43

Ferch J, Granitza B, Masche C and Raith W 1985 *J. Phys. B: At. Mol. Phys.* **18** 967-83

Fon W C, Berrington K A, Burke P G and Hibbert A 1983 *J. Phys. B: At. Mol. Phys.* **16** 307-21

Fon W C, Berrington K A and Hibbert A 1984 *J. Phys. B: At. Mol. Phys.* **17** 3279-94
Haberland R, Fritsche L and Noffke J 1986 *Phys. Rev.* A **33** 2305-14
Jost K, Bisling P G F, Eschen F, Felsmann M and Walthar L 1983 *Proc. 13th Int. Conf. on the Physics of Electronic Atomic Collisions, Berlin* ed J Eichler *et al* (Amsterdam: North-Holland) p 91
—— 1984 Unpublished and private communication
Kauppila W E, Stein T S and Jesion G 1976 *Phys. Rev. Lett.* **36** 580-4
Kauppila W E, Stein T S, Jesion G, Dababneh M S and Pol V 1977 *Rev. Sci. Instrum.* **48** 822-8
Kumar V, Krishnakumar E and Subramanian K P 1987 *J. Phys. B: At. Mol. Phys.* **20** 2899-910
McEachran R P and Stauffer A D 1983 *J. Phys. B: At. Mol. Phys.* **16** 4023-38
—— 1984 *J. Phys. B: At. Mol. Phys.* **17** 2507-18
Nickel J C, Imre K, Register D F and Trajmar S 1985 *J. Phys. B: At. Mol. Phys.* **18** 123-33
Sin Fai Lam L T 1982 *J. Phys. B: At. Mol. Phys.* **15** 119-42